

# Journal of Materials Chemistry A

Accepted Manuscript



This article can be cited before page numbers have been issued, to do this please use: D. A. Nowicki, J. Skakle and I. Gibson, *J. Mater. Chem. A*, 2018, DOI: 10.1039/C7TA09334A.



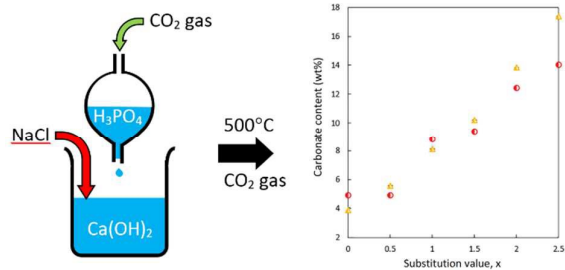
This is an Accepted Manuscript, which has been through the Royal Society of Chemistry peer review process and has been accepted for publication.

Accepted Manuscripts are published online shortly after acceptance, before technical editing, formatting and proof reading. Using this free service, authors can make their results available to the community, in citable form, before we publish the edited article. We will replace this Accepted Manuscript with the edited and formatted Advance Article as soon as it is available.

You can find more information about Accepted Manuscripts in the [author guidelines](#).

Please note that technical editing may introduce minor changes to the text and/or graphics, which may alter content. The journal's standard [Terms & Conditions](#) and the ethical guidelines, outlined in our [author and reviewer resource centre](#), still apply. In no event shall the Royal Society of Chemistry be held responsible for any errors or omissions in this Accepted Manuscript or any consequences arising from the use of any information it contains.

## Nowicki, Skakle and Gibson: Table of Contents entry



A novel approach to carbon sequestering using hydroxyapatite to incorporate significant amounts of  $\text{CO}_2$  with potential product applications as fertiliser.



## Nano-Scale Hydroxyapatite Compositions for the Utilization of CO<sub>2</sub> Recovered Using Post-Combustion Carbon Capture

Duncan A. Nowicki<sup>a</sup>, Janet M. S. Skakle<sup>a,b</sup> and Iain R. Gibson<sup>a,c</sup>

Received 00th January 20xx,  
Accepted 00th January 20xx

DOI: 10.1039/x0xx00000x

[www.rsc.org/](http://www.rsc.org/)

**Abstract:** The synthesis and analysis of a sodium-carbonate co-substituted hydroxyapatite (Ca<sub>10-x</sub>Na<sub>x</sub>(PO<sub>4</sub>)<sub>6-x</sub>(CO<sub>3</sub>)<sub>x</sub>(OH)<sub>2</sub>) with potential applications in carbon capture technologies is described. A co-substituted hydroxyapatite, using NaCl as the source of sodium, containing approximately 14 wt% carbonate was successfully prepared by an aqueous precipitation reaction followed by a thermal treatment under a stream of CO<sub>2</sub> gas at 500°C. In order to reach this level of carbonation, CO<sub>2</sub> gas was constantly supplied to the reactant mixture during precipitation. Another hydroxyapatite prepared with sodium carbonate, Na<sub>2</sub>CO<sub>3</sub>, in non-carbonated water but following the same methodology, incorporated a higher level (approximately 17 wt%) of carbonate. This increase was likely a result of additional carbonate provided by the sodium carbonate starting material. The underlying aim of this work was to examine the possibility of using hydroxyapatites to incorporate carbon dioxide from gas recovered from post-combustion carbon capture (PC-CC) techniques. As the chemical composition of these materials resembles bone mineral, it may be possible to use the final product in agriculture as a slow-release fertilizer and thus make use of the products.

### 1. Introduction

The effect which increasing levels of carbon dioxide is having on the earth's climate is of worldwide concern. An IPCC report from 2014 stated that CO<sub>2</sub> comprises roughly 65% of total greenhouse gas emissions<sup>1</sup>, arising predominantly from fossil fuel powered electricity generation<sup>2</sup>. An aggressive approach to reduce the emission of this gas is thus required to help address climate change. One of the most developed methods for reducing emissions of CO<sub>2</sub> from these sources is termed flue gas separation or post-combustion carbon capture (PC-CC), where CO<sub>2</sub> is stripped from a flue gas stream comprised of various components such as air, water vapour and CO<sub>2</sub>, amongst others, using materials such as amines or solid calcium-based sorbents<sup>3-7</sup> prior to that stream's expulsion to the wider environment. However, instead of simply sequestering the separated CO<sub>2</sub> in a reservoir such as an exhausted oil field, recent attention has focussed instead on utilising this gas in the production of useful materials, with the secondary benefit of enhancing the economics of the carbon capture process itself by offsetting some of the capital and operating costs. For example, a waste processing and energy generation company in

the Netherlands developed a process<sup>8</sup> whereby the CO<sub>2</sub> generated from the combustion of waste was used in the mineralisation of sodium hydrogen-carbonate (NaHCO<sub>3</sub>) from a saturated solution of sodium carbonate (Na<sub>2</sub>CO<sub>3</sub>), producing a slurry containing 40 wt% NaHCO<sub>3</sub>. This slurry was later used to remove acidic impurities from the waste combustion flue gas stream itself. Not only did this slurry outperform solid NaHCO<sub>3</sub> particles, it reduced the emission of CO<sub>2</sub> from the plant by 2000 tons/year<sup>8</sup>. Another example of combining CO<sub>2</sub> capture with the formation of a product with a clear technical application is using Mg-brines combined with CO<sub>2</sub> resulting in precipitation of a magnesium-hydroxy-carbonate-hydrate (MHCH) phase, which contained at least 30 wt% of CO<sub>2</sub> and could have applications as a cement<sup>9</sup>.

In a similar manner, CO<sub>2</sub> gas could be utilised in the synthesis of a single-phase carbonated hydroxyapatite. This could act as a route to both 'lock' away carbon dioxide gas into a solid material whilst also having beneficial applications. Hydroxyapatite, HA, (Ca<sub>10</sub>(PO<sub>4</sub>)<sub>6</sub>(OH)<sub>2</sub>) is a widely-studied and adaptable calcium phosphate material. The hydroxyapatite lattice can accommodate a large quantity of carbonate (the carbonate content of bone mineral is in the range of 4-8 wt%<sup>10</sup>) owing to its ability to substitute both hydroxyl (OH) and phosphate (PO<sub>4</sub>) groups for carbonate (CO<sub>3</sub>) groups. This is achieved through chemical substitution mechanisms, termed A-type and B-type substitution respectively<sup>11</sup>. A-type substitution can be attained by heating the apatite in an atmosphere of CO<sub>2</sub> and has a theoretical maximum substitution level. The substitution of phosphate groups for carbonate groups can be achieved by the synthesis of a phosphate-deficient apatite (Ca/P > 1.67) with

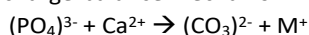
<sup>a</sup> Department of Chemistry, University of Aberdeen, Meston Walk Aberdeen AB24 3UE.

<sup>b</sup> Department of Physics, University of Aberdeen, Meston Walk Aberdeen AB24 3UE.

<sup>c</sup> Institute of Medical Sciences, University of Aberdeen, Foresterhill, Aberdeen AB25 2ZD.

Electronic Supplementary Information (ESI) available: [details of any supplementary information available should be included here]. See DOI: 10.1039/x0xx00000x

concomitant carbonate substitution introduced through the water used in the aqueous synthesis and/or the calcining/sintering atmosphere<sup>12</sup>. To maintain charge balance this substitution also requires equimolar substitution of carbonate ions for hydroxyl ions. This substitution mechanism therefore has a limit on the maximum level of carbonate substitution as it relies on the limiting A-type substitution. The traditional synthesis mechanism for substituting carbonate ions into the hydroxyapatite lattice is by co-substitution of carbonate with a monovalent cation, typically sodium ions<sup>13,14</sup> but also ammonium<sup>15</sup> or potassium ions<sup>16</sup>. In these examples some of the calcium ions are substituted for e.g. sodium ions, allowing more carbonate to be incorporated into the structure, according to the charge-balance mechanism:



where  $\text{M}^+$  can be  $\text{Na}^+$ ,  $\text{NH}_4^+$ , or  $\text{K}^+$ . This gives the substitution mechanism  $\text{Ca}_{10-x}\text{M}_x(\text{PO}_4)_{6-x}(\text{CO}_3)_x(\text{OH})_2$ .

The wide availability and low cost of sodium chloride made it an attractive choice to use as the source of these co-substituting cations in this work over another more expensive reagent. Moreover, with further development it may be possible to utilise sea water directly in the synthesis of this material although this would present its own challenges due to the presence of other dissolved ions that may substitute into the apatite. There is extensive research on the substitution of sodium ions into the hydroxyapatite lattice in pursuit of a high-quality bone replacement material, but little specifically using NaCl in the preparation of the apatite. Sodium-carbonate co-substituted hydroxyapatite, with sodium and carbonate contents in the typical range of bone mineral, was prepared by soaking HA prepared from calcium carbonate ( $\text{CaCO}_3$ ) and ortho-phosphoric acid ( $\text{H}_3\text{PO}_4$ ) in a solution of  $\text{NaHCO}_3$  at 60 °C<sup>17</sup>. The researchers reported that the carbonate content of the apatites increased alongside the sodium content. Apatites with no sodium substitution displayed a carbonate content of 1.3 wt%; this rose to a maximum of 6.0 wt% when the degree of sodium incorporation rose to 1.5 wt%, with the vast majority (94%) of this carbonate situating on the B-site<sup>17</sup>. Stephen *et al.* substituted sodium ions into the HA structure by way of an aqueous precipitation reaction. In their study, compositions of single-phase sodium-carbonate co-substituted HA with substitution values of  $x=0.32$  and Ca/P ratios of 1.70 were prepared using either  $\text{Na}_2\text{CO}_3$  or  $\text{NaHCO}_3$  as the source of the sodium and carbonate co-substituting cations. Their preparations were designed in such a way that carbonate would substitute onto the hydroxyl and phosphate sites so the overall (Ca+Na)/(P+C) ratio was 1.67, i.e. that of a stoichiometric HA. These precipitates were subsequently sintered at 900 °C in an atmosphere of  $\text{CO}_2$  and  $\text{H}_2\text{O}$ . Afterward, the carbonate contents of these compositions were estimated by heating the samples at 1300 °C for 24 hours in air and measuring the mass loss. Although the extent of B-type substitution (the magnitude of the  $x$ -value) was designed to be the same no matter which sodium reagent was used, the sample precipitated using  $\text{Na}_2\text{CO}_3$

had higher carbonate content than the sample prepared using  $\text{NaHCO}_3$ , assuming this mass loss was entirely due to  $\text{CO}_2$ . While the use of  $\text{Na}_2\text{CO}_3$  could provide sources of both sodium and carbonate ions to try to maximise the carbonate incorporation in apatite compositions, it would be beneficial to have the versatility to achieve high degrees of carbonation without the need to introduce this carbonate-containing reagent into the reactant mixture. This would widen the number of routes available for carbonate incorporation into the apatite structure by employing carbonate-free reagents during the synthesis and therefore focussing on the introduction of carbonate solely from gas sources,

The aim of the present work, therefore, was to investigate whether high levels of carbonation of HA could be achieved using sodium chloride (NaCl) as the source of sodium ions, with carbonate ions being introduced by addition of  $\text{CO}_2$  gas into the precipitation reaction and also during calcining. Analysis of these precipitated and heated samples allowed an evaluation of the most favourable conditions for the carbonation of the co-substituted apatite to be made.

## 2. Experimental

### 2.1. Sample Preparation

Sodium-carbonate co-substituted hydroxyapatite compositions were synthesised at room temperature according to the above formula  $\text{Ca}_{10-x}\text{M}_x(\text{PO}_4)_{6-x}(\text{CO}_3)_x(\text{OH})_2$ . The method was based on an established aqueous precipitation method that involved adding a phosphoric acid solution dropwise to an aqueous suspension of calcium hydroxide<sup>18</sup> with substitution values of  $0.5 \leq x \leq 3.0$  (in the above formula) using NaCl as the source of sodium ions in the reactant mixture. This mechanism focuses on balancing charge on the calcium and phosphate sites of HA, with any carbonate for hydroxyl substitution considered to occur independently. Three series of apatites were precipitated using each reagent; each series was identical except for the variable of the introduction of  $\text{CO}_2$  gas into the phosphate solution reactant. The three were as follows:

- 1) No  $\text{CO}_2$  gas was used in the first series, named "No  $\text{CO}_2$ ".
- 2)  $\text{CO}_2$  gas was bubbled into the phosphate reactant solution for approximately 30 minutes (until the pH approached pH=4) prior to the start of addition of this solution to the  $\text{Ca}(\text{OH})_2$  suspension. This was named " $\text{CO}_2$ -I".
- 3)  $\text{CO}_2$  gas was bubbled into the phosphate solution throughout the addition of this to the  $\text{Ca}(\text{OH})_2$  suspension. The dissolution of the  $\text{CO}_2$  gas into the water and subsequent evolution of carbonate ( $\text{CO}_3$ ) and hydrogen-carbonate ( $\text{HCO}_3$ ) groups did not affect the temperature of the phosphate solution and by extension the reactant mixture to any significant extent. This was named " $\text{No-CO}_2$ -ii".

A calcium + sodium suspension was prepared by dissolving NaCl (>99.5% assay, Fisher Scientific, UK) followed by dispersing  $\text{Ca}(\text{OH})_2$  (98% assay, VWR, UK) in approximately 150 ml of

distilled water, while mixed with a magnetic stirrer. Concentrated ammonium hydroxide solution (30 ml) was added to this suspension to ensure that the pH did not fall below an acceptable limit (pH=9-11) to avoid the formation of calcium-deficient impurity phases<sup>19,20</sup> upon the introduction of the phosphoric acid solution. The phosphate solution was prepared by diluting ortho-phosphoric acid, H<sub>3</sub>PO<sub>4</sub>, (85% assay, Fisher Scientific, UK) with approximately 150 ml of distilled water. Depending on the series that was being synthesised, if required CO<sub>2</sub> gas was then bubbled into this solution, as described above. Whilst the calcium-sodium suspension was placed under constant stirring in order to avoid the formation of brushite or monetite<sup>20,21</sup>, the phosphate solution was added dropwise over a timescale of about 2 hours. This also prevents any significant heat being produced through exothermic reaction. After the complete addition of the acid, the stirring was maintained for a further two hours and then the precipitate was aged overnight. The precipitate was filtered under vacuum and rinsed with distilled water. The resultant filter-cake was dried in an oven at 90°C then ground to a fine powder using a mortar and pestle. To further increase the carbonate content of the apatites, the precipitates of the series which reached the highest level of substitution (CO<sub>2</sub>-ii) before the rise of any secondary phases by XRD were subsequently heated in a carbon dioxide atmosphere at 500 °C. Aliquots (~0.5 g) were heated in a tube furnace (Model: CFS 12/3, Carbolite Gero Ltd., UK) under a CO<sub>2</sub> gas flow rate between 0.2-0.3 dm<sup>3</sup> per minute. Samples were heated from room temperature to 500 °C at 5 °C/min, held there for one hour and then cooled back down to room temperature at 5°C/min.

## 2.2. Sample Characterisation

Powder X-ray Diffraction (XRD) was carried out to determine the phase composition of the powders using an X'Pert Pro diffractometer (PANalytical Ltd., UK) with Cu K<sub>α</sub> radiation (λ=1.5418 Å), collecting data over a 2θ range of 15-65 ° with a step size of 0.013 ° and a count time of 95 s. The X-ray generator operated at 45 kV and 40 mA. Crystalline phases present were identified using PDF files from the ICDD database: HA (#26-204), aragonite (#56-090) and calcite (#28-827). The unit cell parameters of the heated apatites were determined by performing a LeBail fit on the obtained XRD patterns using HighScore Plus software. These fits were based on the HA structural data reported by Sudarsanan and Young<sup>22</sup>, using the space group P6<sub>3</sub>/m. Only the background, lattice parameters and the peak shapes were refined.

FT-IR spectra were obtained using a Diamond/ZnSe ATR attached to a Spectrum Two™ (Perkin-Elmer, UK) spectrometer. These absorbance spectra were collected at a 2 cm<sup>-1</sup> resolution averaging 8 scans between wavenumbers of 4000 cm<sup>-1</sup> and 400 cm<sup>-1</sup>.

The carbonate contents of the samples were determined by combustion infrared analysis using a CS744 Series LECO carbon/sulphur analyser (LECO Instruments UK Ltd., UK); for each sample duplicate measurements were made and the mean

value reported. Two assumptions were made in the interpretation of carbon analysis in terms of reporting carbonate contents. Firstly, it was assumed that all of the carbon detected by the equipment was present as CO<sub>2</sub> which is reasonable as the equipment flooded the sample with oxygen, ensuring complete combustion. The second was that any carbon existed in the apatite structure exclusively as carbonate ions, again quite reasonable. Mixtures of stoichiometric HA and calcium carbonate were prepared to produce samples with known carbon contents; testing of these confirmed that the analyser was accurate and precise.

## 3. Results and Discussion

### 3.1. As-prepared apatites

XRD analysis (Figure 1) was used to determine the phase composition of the as-prepared powders to investigate the effect the introduction of CO<sub>2</sub> gas into the phosphate solution had on the phase compositions of the apatite precipitates. Each obtained pattern matched the ICDD standard for hydroxyapatite (PDF #26-204), confirming the synthesis of a sodium-carbonate co-substituted HA which remained the major phase throughout. Relatively broad diffraction peaks were seen in each pattern, indicating the precipitation of an apatite phase made up of very small hydroxyapatite crystallites<sup>23</sup>. Some of the diffraction peaks moved with rising x-values, revealing changes in the d-spacing and the dimensions of the unit cells as will be discussed below. The compositions of the CO<sub>2</sub>-ii series remained phase-pure by XRD for substitution values up to and including x=2.5, the same value that was reached when a carbonate-containing reagent (Na<sub>2</sub>CO<sub>3</sub>) was used as the source of sodium ions (data not shown). However, this limit of substitution fell to x=1.0 and x=1.5 in the No-CO<sub>2</sub> and CO<sub>2</sub>-i series respectively. Above these limits, small quantities of calcium carbonate were seen to precipitate alongside the apatite phase, initially as aragonite and then as a combination of aragonite and calcite at higher substitution levels; diffraction peaks corresponding to each of these secondary phases are highlighted in Figure 1. There is evidence in the literature that suggests the presence of chloride ions in the reactant mixture may influence the precipitation of aragonite<sup>24</sup>. For these compositions in the No-CO<sub>2</sub> and CO<sub>2</sub>-i series it is likely that there is insufficient carbonate in the reactant mixture to support co-substitution in the apatite phase, so the calcium-rich composition favours formation of calcium carbonate phases. In the CO<sub>2</sub>-ii series, excess carbonate ions would be present by the constant bubbling of CO<sub>2</sub> gas into the phosphate reactant throughout the addition of this solution to the reactant mixture. This would provide sufficient carbonate ions to maintain co-substitution even for high values of x. Normalised FTIR spectra between 1800-400 and 4000-3400 cm<sup>-1</sup> for the as-prepared powders of each series are shown in Figure 2. Figure 2(a, c, e) displays the characteristic ν<sub>1</sub>, ν<sub>2</sub>, ν<sub>3</sub> and ν<sub>4</sub> phosphate bands at approximately 962 cm<sup>-1</sup>, 474 cm<sup>-1</sup>, 1020-1090 cm<sup>-1</sup> and 570-600 cm<sup>-1</sup>, respectively, corresponding to



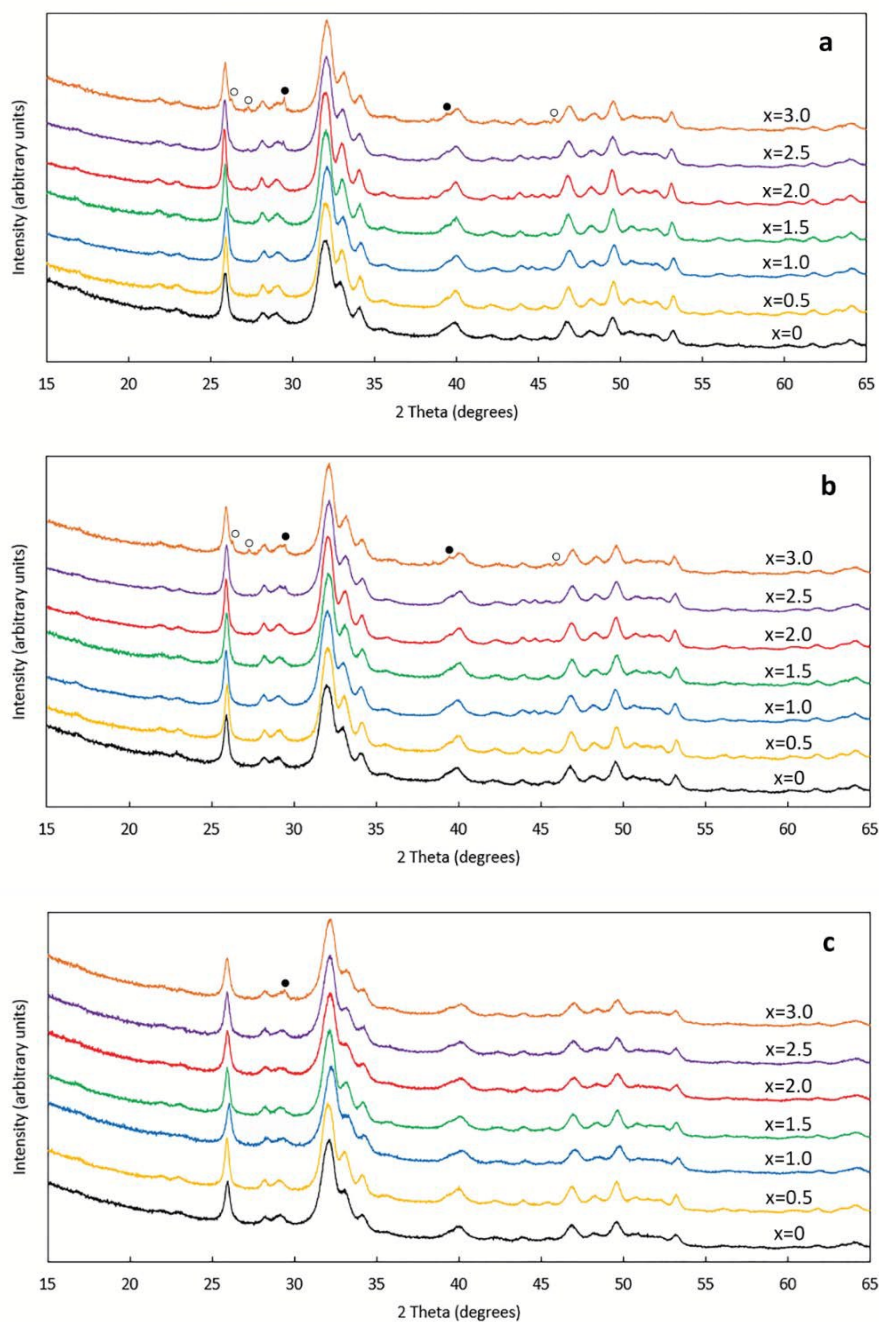


Figure 1: Normalised X-ray diffraction patterns of dried, as-prepared apatites precipitated using NaCl with substitution values ranging from  $x=0.5$  to  $x=3.0$  and differing phosphate solution conditions (a) No- $\text{CO}_2$ , (b)  $\text{CO}_2$ -i and (c)  $\text{CO}_2$ -ii. Peaks corresponding to aragonite (o) and calcite (●) are marked accordingly

to synthetic hydroxyapatite<sup>25,26</sup>, which were observed in each sample.

Each of these bands remained clearly resolved even at the highest substitution values. Additionally, a shoulder on the left-hand side of the  $\nu_4$  phosphate band at 630-640  $\text{cm}^{-1}$ , corresponding to an OH librational vibration, was observed at low  $x$ -values in all three series. However it progressively decreased in intensity as the degree of substitution rose, almost disappearing in the  $\text{CO}_2$ -ii series as the limit of substitution was approached. This decrease in intensity may be associated with

increasing carbonate-for-hydroxyl substitution on the A-site of the apatite structure, as has been observed by Rehman and Bonfield<sup>25</sup>. An OH stretch band around 3570  $\text{cm}^{-1}$  was also observed (see Figure 2(b, d, f)) at low levels of substitution, particularly in apatites of the No- $\text{CO}_2$  series, behaving in the same manner as the OH libration peak, again likely a consequence of carbonate substitution.  $\nu_2$  and  $\nu_3$  carbonate bands situated between 870-880  $\text{cm}^{-1}$  and 1300-1600  $\text{cm}^{-1}$  respectively were also present in every spectra shown in Figure 2(a, c, e), increasing in intensity with the  $x$ -value in each series.

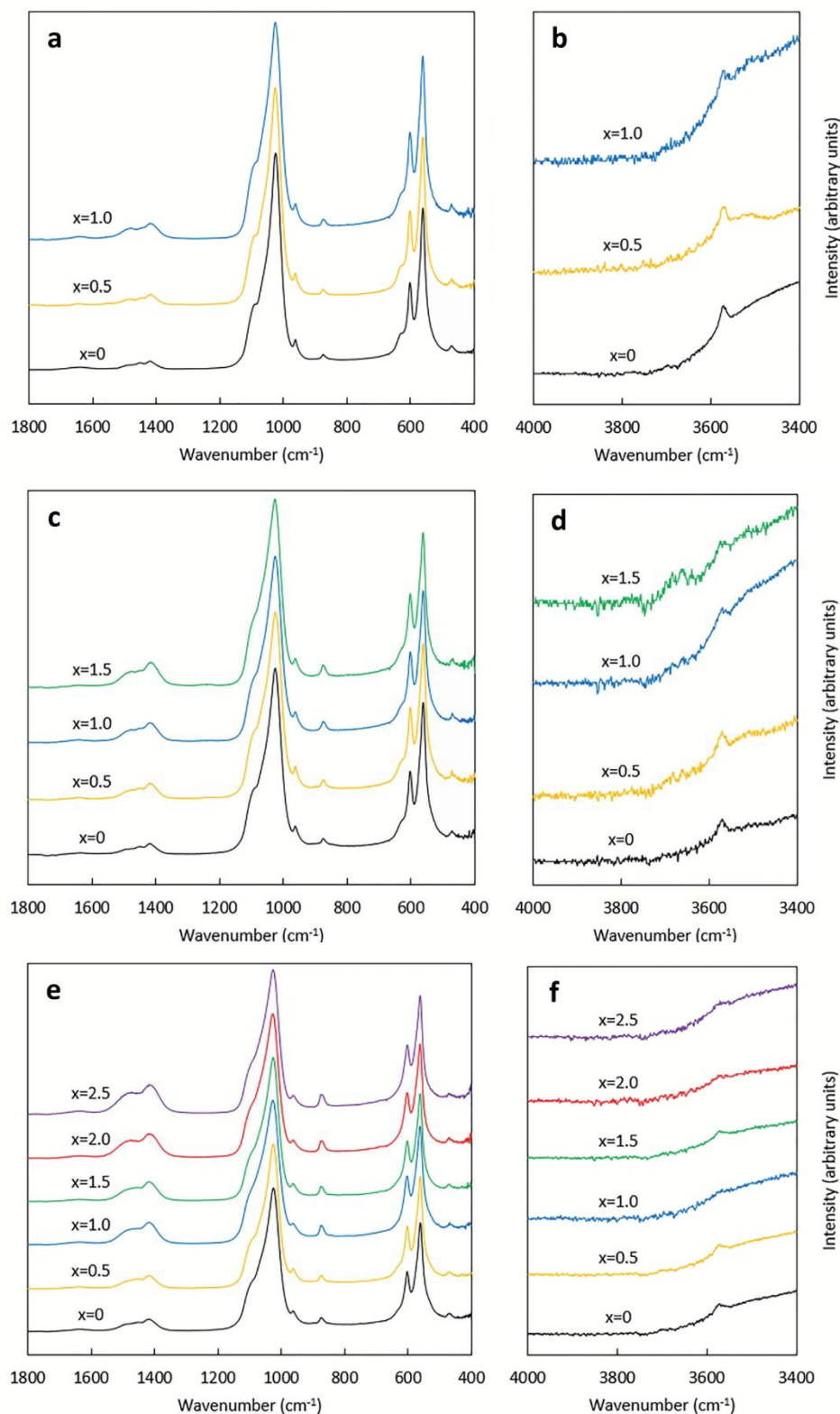


Figure 2: Normalised FT-IR absorbance spectra of as-prepared apatites precipitated using NaCl as the source of sodium ions with substitution values between  $x=0.5$  and  $x=2.5$  and differing phosphate solution conditions (a, b) No- $\text{CO}_2$ , (c, d)  $\text{CO}_2$ -i and (e, f)  $\text{CO}_2$ -ii. Only single-phase samples were presented here.

Deduction of the relative location of substituted carbonate groups in as-precipitated compositions of HA is problematic as an  $\text{HPO}_4$  vibration<sup>26,27</sup> has been reported at about  $875\text{ cm}^{-1}$ . The apatites of the  $\text{CO}_2$ -ii series displayed the most intense of these carbonate bands. Figure 3, which compares the intensity of these carbonate bands across each series at a substitution value of  $x=1.0$ , illustrates the significant effect that bubbling  $\text{CO}_2$  gas into the phosphate solution had on the intensity of these bands.

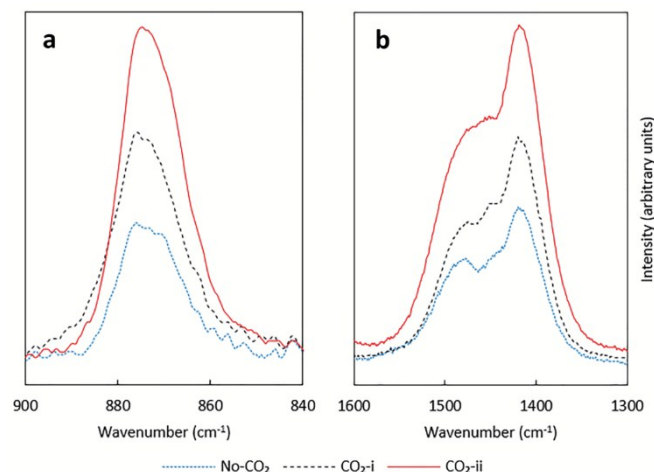


Figure 3: Normalised FT-IR spectra between  $900\text{--}840\text{ cm}^{-1}$  and  $1600\text{--}1300\text{ cm}^{-1}$  displaying the (a)  $\nu_2$  and (b)  $\nu_3$  carbonate bands of as-prepared apatites precipitated using differing phosphate solution conditions No- $\text{CO}_2$ ,  $\text{CO}_2$ -i and  $\text{CO}_2$ -ii at a substitution value of  $x=1.0$ .

It is clear that introducing additional carbonate ions into the phosphate solution led to an increase in the intensity of these bands. Whilst a modest increase in intensity was seen when  $\text{CO}_2$  was bubbled into the phosphate solution for only thirty minutes ( $\text{CO}_2$ -i), it was when  $\text{CO}_2$  was bubbled in continuously ( $\text{CO}_2$ -ii) that the intensity of these bands increased significantly. It should be noted that for the No- $\text{CO}_2$  series, in which no  $\text{CO}_2$  was intentionally added to the reactant mixture at any time, low intensity carbonate vibrations were observed for all values of  $x$ . These syntheses were performed in air, and samples were aged and dried in air, providing opportunities for some atmospheric  $\text{CO}_2$  to be incorporated into the reaction.

Figure 4 presents values for the quantitative analysis of carbonate contents of the as-prepared powders. In each series of apatites, the carbonate contents were seen to rise linearly with the substitution value,  $x$  (the value obtained for the  $x=1.0$  precipitate of the  $\text{CO}_2$ -ii series was considered to be an outlier with the  $\text{CO}_3$  substitution into the  $x=0$  sample of the same series likely occurring *via* a different mechanism than when potassium was co-substituted into the structure). Failing to bubble  $\text{CO}_2$  gas into the phosphate solution during precipitation (No- $\text{CO}_2$  series) led to a maximum carbonate content of 3.5 wt% when  $x=1.0$ . This carbonate most likely originated from atmospheric carbon dioxide that had dissolved into the reactant mixture. The

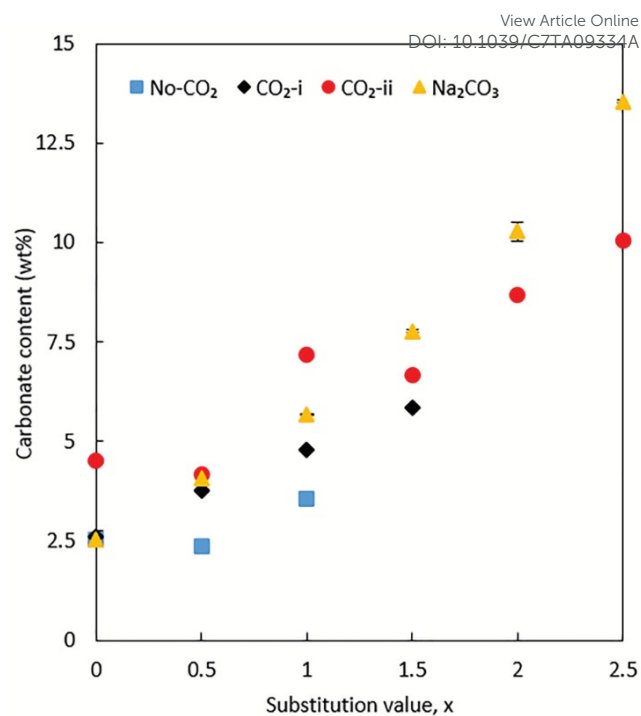


Figure 4: Carbonate contents of the as-prepared apatites with substitution values between  $x=0.5$  and  $x=2.5$ , precipitated under each condition. Only single-phase samples are presented here. Carbonate contents of apatites precipitated using  $\text{Na}_2\text{CO}_3$  in non-carbonated water are also presented.

apatites precipitated using  $\text{CO}_2$  gas, regardless of the timescale of supply ( $\text{CO}_2$ -i and  $\text{CO}_2$ -ii), showed higher carbonate contents at every  $x$ -value when compared to their counterparts synthesised without the introduction of this gas (No- $\text{CO}_2$ ). Initially the difference in the carbonate content between apatites of the  $\text{CO}_2$ -i and  $\text{CO}_2$ -ii series was small. For example, when  $x=0.5$ , continuously bubbling  $\text{CO}_2$  gas into the phosphate solution resulted in a carbonate content of only 4.2 wt%, compared to 3.8 wt% when this gas was bubbled in only prior to addition of the phosphate solution to the  $\text{Ca}(\text{OH})_2$  suspension. However, this disparity grew with  $x$ ; when the substitution value was increased to  $x=1.5$ , the carbonate contents were 6.7 wt% and 5.8 wt% for apatites of the  $\text{CO}_2$ -ii and  $\text{CO}_2$ -i series respectively. The highest value of all was seen in the  $\text{CO}_2$ -ii series, 10.0 wt% when  $x=2.5$ , close to three times the maximum carbonate content seen in the No- $\text{CO}_2$  series, demonstrating the importance of bubbling carbon dioxide gas into the phosphate solution when NaCl was used. This apex reached using sodium chloride did fall below the degree of carbonation that was achieved using  $\text{Na}_2\text{CO}_3$ ; a single-phase apatite with 13.5 wt% carbonate was prepared in non-carbonated water using that carbonate-containing reagent as the source of sodium ions. Therefore, it is clear that bubbling  $\text{CO}_2$  gas into the phosphate solution continuously is essential to maximise the degree of carbonation of hydroxyapatite when NaCl was used, and to approach the level obtained for co-substitution with addition of  $\text{Na}_2\text{CO}_3$ .



### 3.2. Heated apatites

Figure 5 shows XRD patterns obtained from the apatites of the CO<sub>2</sub>-ii series, after being heated at 500°C in a carbon-dioxide atmosphere. All of the samples still matched the PDF standard for hydroxyapatite, with no secondary phases formed as a result of the thermal treatment.

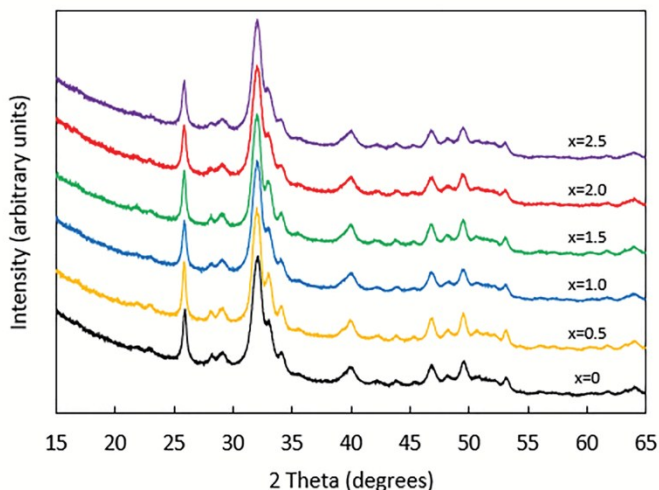


Figure 5: XRD patterns of the apatites of the CO<sub>2</sub>-ii series after being heated at 500°C under a stream of CO<sub>2</sub> gas.

The diffraction peaks remained quite broad as might be expected for the low temperatures used, the apatites remaining poorly crystalline with small crystallite sizes. The Scherrer equation<sup>28</sup> (Equation 1), was used to evaluate the size of the crystallites after heating relative to their as-prepared counterparts, assuming any strain in the lattice had a negligible effect on the line broadening:

$$t = \frac{0.9\lambda}{B\cos\theta}$$

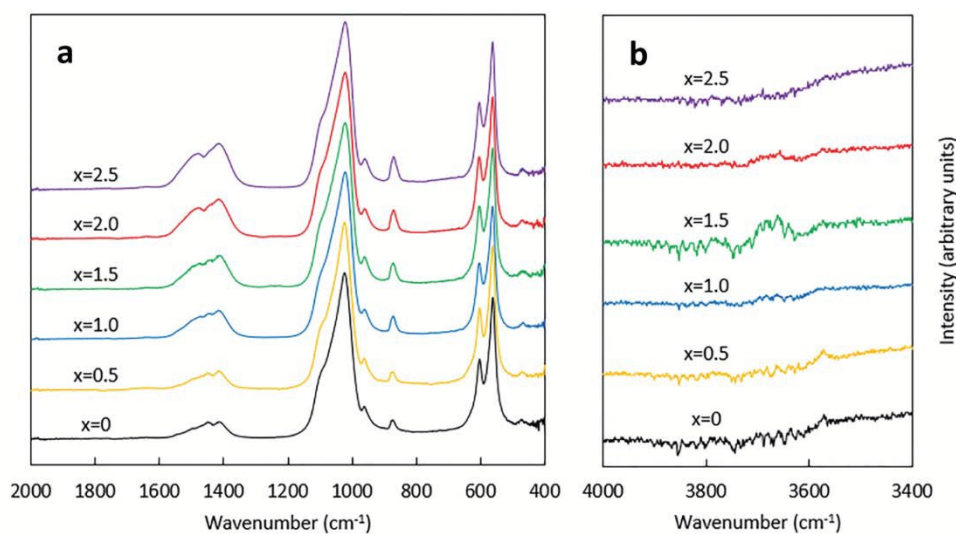


Figure 3: FT-IR spectra between (a) 2000-400 cm<sup>-1</sup> and (b) 4000-3400 cm<sup>-1</sup> of heated apatites (500°C in CO<sub>2</sub> atmosphere) of the CO<sub>2</sub>-ii series.

where  $\tau$  is the mean crystallite size in nanometres,  $\lambda$  the wavelength of the CuK $\alpha$  incident radiation,  $\theta$  the Bragg angle and  $B$  is the relative peak width where  $B^2 = B_M^2 - B_S^2$ .  $B_M$  is the full-width at half maximum (FWHM) in radians of the chosen peak (the (002) reflection near 25° in this case) and  $B_S$  is the instrumental line broadening, measured from the 111 peak of a silicon standard at  $2\theta = 28.44^\circ$ . Heating the precipitates in a CO<sub>2</sub> atmosphere led to slightly (but consistently) smaller apatite crystallites relative to the precipitates (see Table 1), likely a function of further carbonate incorporation into the structure from the thermal treatment. It should be noted that use of the (002) peak only represents one dimension of the crystals, which tend to be acicular<sup>28</sup>.

Table 1: Crystallite sizes (nm) of apatites as-prepared (using CO<sub>2</sub>-ii method) and after being heated at 500°C in CO<sub>2</sub>

x	As-prepared	Heated at 500°C
0	25.4	23.4
0.5	28.3	26.7
1.0	22.3	21.0
1.5	27.2	25.5
2.0	23.3	21.7
2.5	24.2	21.1

As can be seen from the FT-IR spectra between 2000-400 cm<sup>-1</sup> in Figure 6(a), the heated apatites again displayed all of the characteristic phosphate peaks previously described for the spectra of as-prepared samples, ostensibly unaffected by the thermal treatment. The OH libration band, seen in the spectra of as-prepared samples as a faint shoulder on the  $\nu_4$  phosphate band, further decreased in intensity after the thermal treatment, likely caused by additional OH-for-CO<sub>3</sub> substitution<sup>12</sup>.

Although the OH stretching bands appeared quite weakly in the precipitates of these apatites, the heat treatment effectively caused them to disappear above a substitution value of  $x=0.5$ , evidenced by the spectra between  $4000-3400\text{ cm}^{-1}$  in Figure 6(b). Like the precipitates, the intensity of the  $\nu_2$  and  $\nu_3$  carbonate bands of the heated compositions increased with rising  $x$ -value. It is likely that there is significant carbonate substitution on the phosphate site (B-type) upon precipitation, originating from the  $\text{CO}_2$  gas that was provided to the reactant mixture, therefore many of the changes on heating the samples in the  $\text{CO}_2$  atmosphere will be related to carbonate substituting on the hydroxyl site (A-type) or being incorporated but not existing on an atomic site in the HA structure (labile).

Analysis of the relative intensities of the peaks (Figure 7) that comprise the  $\nu_2$  carbonate band observed by FTIR is a common method for differentiating the type of carbonate that is present in carbonate substituted HA. Fleet<sup>29</sup> reported that the  $\nu_2$  carbonate region provides the clearest idea of the location of these carbonate groups as it avoids the messy, overlapping contributions that comprise the  $\nu_3$  carbonate region between  $1400\text{ cm}^{-1}$  and  $1600\text{ cm}^{-1}$ .

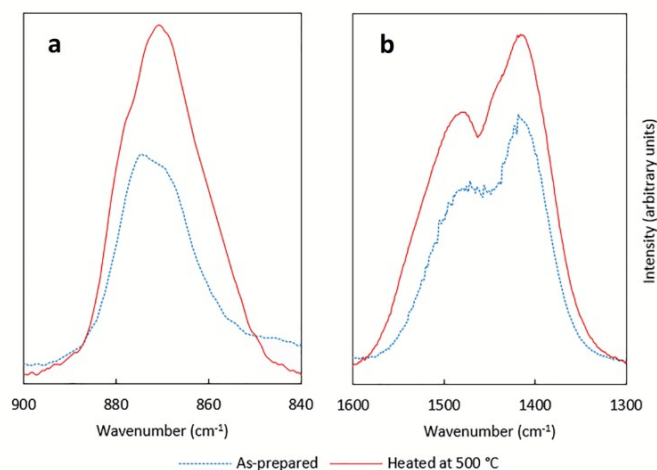


Figure 7: FT-IR spectra of the apatites of the  $\text{CO}_2$ -ii between (a)  $900-840\text{ cm}^{-1}$  and (b)  $1600-1300\text{ cm}^{-1}$  displaying the  $\nu_2$  and  $\nu_3$  carbonate bands respectively of the as-prepared (AP) and heated ( $500^\circ\text{C}$  in  $\text{CO}_2$  atmosphere) apatites where  $x=2.5$ .

Upon precipitation a broad peak centred at  $874\text{ cm}^{-1}$ , with peak asymmetry to either side of this, was obtained with poor definition of distinct vibrations that may be assigned to A-type, B-type or labile carbonate. Additionally, as has been mentioned, the contribution from probable  $\text{HPO}_4$  groups in this region made the separation and assignment of these peaks even more difficult. Heating likely brought about the dehydration of these groups<sup>30</sup> and the corresponding disappearance of the  $\text{HPO}_4$  band at  $875\text{ cm}^{-1}$ <sup>27</sup>, improving the peak resolution of the  $\nu_2$  vibration, with a peak at high wavenumber ( $\sim 880\text{ cm}^{-1}$ ) appearing more distinct from the peak with maximum intensity at  $\sim 871\text{ cm}^{-1}$ . However, from the spectra of the heated apatite in Figure 7(a), it does appear that the majority of the carbonate present was still situated on the

B-site. Although not used in the determination of the location of the carbonate groups in the apatite, it is worth noting that the profile of the  $\nu_3$  carbonate band (Figure 7(b)), also changed markedly after being exposed to the thermal treatment, with a peak about  $1480\text{ cm}^{-1}$  and a shoulder on the left of the peak near  $1415\text{ cm}^{-1}$  appearing more prominently. The measured carbonate contents of the heated apatites are presented in Figure 8. As was the case with the as-prepared powders, there was a quasi-linear relationship between the substitution value and the resultant carbonate content of the apatite.

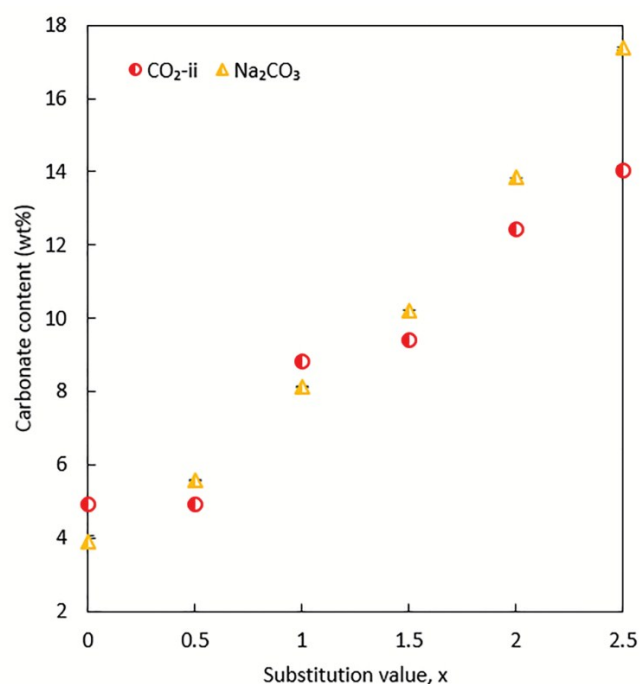


Figure 8: Carbonate contents of the apatites of the  $\text{CO}_2$ -ii series after being heated at  $500^\circ\text{C}$  under a  $\text{CO}_2$  stream. The carbonate contents of apatites precipitated using  $\text{Na}_2\text{CO}_3$  in non-carbonated water after being heated in the same fashion are presented for comparison..

Each of the compositions displayed a higher carbonate content after being exposed to the thermal treatment in the carbon dioxide atmosphere. The maximum carbonate content observed for the heated samples precipitated using  $\text{NaCl}$  was  $14.0\text{ wt}\%$  when  $x=2.5$ , however again this fell below the carbonate content of  $17.4\text{ wt}\%$  seen for an apatite precipitated using  $\text{Na}_2\text{CO}_3$  with equal substitution value that had been heated following the same regime. This is a very high level of carbonate substitution in the apatite structure therefore it is likely that the combined substitution of significant amounts of carbonate and sodium will have profound effects on the properties such as the solubility of the material. Although there was a disparity in the carbonate contents of the apatites precipitated using these two reagents at high substitution values, at low levels of substitution the carbonate contents were very similar, diverging after the degree of substitution rose above  $x=1.5$ .

Figueiredo *et al.* reported that calcining hydroxyapatite at 600 °C caused a significant increase in the total porosity of the apatite<sup>31</sup> and so further work should be carried out to optimise the heating conditions to maximise the carbonate content of the apatite, either through direct substitution or adsorption on the surface. Furthermore, precipitating the apatite using NaCl led to the inclusion of some chloride groups in final sample, whether that be as part of the crystal structure or on the surface, evidenced by the poisoning of the halide trap of the equipment used to determine the sample's carbonate content. The development of some procedure to mitigate the presence of this undesirable ion whilst using NaCl is essential to allow for the synthesis of an environmentally safe material. The separated CO<sub>2</sub> which is to be "locked into" the apatite structure could also be used to prepare Na<sub>2</sub>CO<sub>3</sub>, perhaps through some sort of modified Solvay process, which would then be used to precipitate the apatite avoiding the issue of the chloride ions altogether.

De Maeyer *et al.* reported an expression for the estimation of the *c* unit cell parameter of a sodium/carbonate co-substituted HA system as a function of the apatite's carbonate content<sup>32,33</sup>. In their work, only B-type substitution was present however it would be beneficial if an expression could be developed for this system where both mechanisms were exploited in order to maximise carbonation. Unit cell parameters obtained using HighScore Plus software are shown along with unit cell volumes and measured carbonate contents (wt%) in Table 2. Additional substitution values other than the ones already presented were prepared for additional data points.

Table 2: *a* and *c* lattice parameters, carbonate contents (wt%) and unit cell volumes of the heated (500°C under a stream of CO<sub>2</sub>) apatites of the CO<sub>2</sub>-ii series.

<i>x</i>	wt% CO <sub>3</sub>	<i>a</i> / Å	<i>c</i> / Å	<i>V</i> / Å <sup>3</sup>
0	4.92	9.391(3)	6.886(3)	525.91
0.25	3.88	9.402(2)	6.893(2)	527.68
0.50	4.91	9.394(2)	6.893(2)	526.78
0.75	5.64	9.399(2)	6.893(2)	529.34
1.00	8.82	9.390(3)	6.896(3)	526.56
1.50	9.40	9.397(2)	6.897(2)	527.42
2.00	12.43	9.393(3)	6.897(3)	526.97
2.50	14.05	9.392(3)	6.900(3)	527.09

Whilst the *a* parameter showed no clear trend with increasing *x* or wt% CO<sub>3</sub>, the *c* parameter generally increased along with the substitution value (and carbonate content), although the changes in this parameter were quite small. As the effective ionic radii of Na<sup>+</sup> and Ca<sup>2+</sup> are quite close (1.12 and 1.06 Å respectively in 7-fold coordination<sup>34</sup>) it is therefore likely that the increasing carbonate-for-phosphate substitution is influencing this parameter<sup>11,32</sup>. The unit cell volume showed no significant change with increasing *x*. The values obtained for the *c* parameter were plotted against each apatites' respective measured carbonate content as displayed in Figure 9 (the

sample where *x*=0 was not included as the mechanism of CO<sub>2</sub> substitution was likely to be different). Thereafter an expression between these two parameters for this sodium-carbonate co-substituted hydroxyapatite system precipitated using NaCl, with a high level of carbonate incorporation was developed using linear regression.

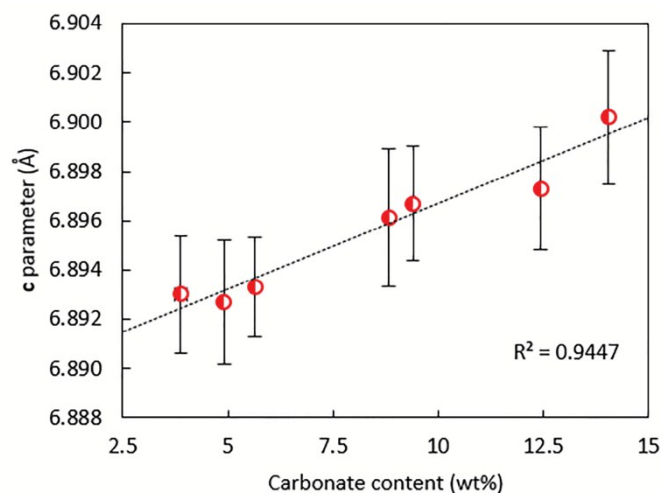


Figure 4: Carbonate contents plotted against *c* unit cell parameters for the heated apatites of the CO<sub>2</sub>-ii series.

This extrapolates back to give unit cell dimensions at *x*=0 for hydroxyapatite which are within experimental error<sup>35,36</sup>. However, there is an inherent error that will be present simply because the analysis was performed using apatites with a wide range of carbonate contents. Additionally, the unit cell parameters were determined using diffraction patterns with quite broad reflections (see Figure 5), adding another degree of uncertainty to the expression. Heating the apatite at significantly higher temperatures would have narrowed the diffraction peaks (increased the crystallite size) but would have led to the formation of impurity phases for many of the compositions. Using a longer dwell time at 500°C may have resulted in a marginal increase in the crystallite size<sup>37</sup> thus producing narrower diffraction peaks but, again, the high levels of carbonation would likely be affected, as carbonate loss from apatite through heating has been demonstrated to be time-dependent<sup>38</sup>.

A reliable equation relating the carbonate content to the *a* lattice parameter, such as those presented by De Maeyer *et al.*<sup>32,33</sup>, could not be developed for the heated apatites in this work. The varying degrees of phosphate-for-carbonate substitution and independent hydroxyl-for-carbonate substitution meant that samples could not be compared like-for-like with regards to trends in the *a* parameter, as A and B-type substitution mechanisms are known to have opposite effects on the unit cell parameters of the apatite. Besides, tightly controlling the extent of A-type substitution between successive heat treatments can be problematic<sup>12</sup>, whether that be caused by the formation of vacancies on the A-site, changes in the flowrate of CO<sub>2</sub> gas into the furnace or perhaps the loss

of other species such as lattice water between 250-300 °C and 300-400 °C causing a change in the *a* parameter not directly caused by the substitution of carbonate<sup>39</sup>. It is a combination of all of these factors which lead to incredibly scattered data and thus a poorly fitting trend line, which would not have produced a substantial relationship.

The present study utilised a gas source that contained 100% CO<sub>2</sub> and if a process based on the results described here was to be utilised in capturing CO<sub>2</sub> from power plant waste gas a number of considerations would need to be studied. In particular, waste gas would contain significantly less CO<sub>2</sub> than the pure gas used here. Additionally, the feasibility of capturing carbonate with a precipitation reaction using a batch process may not be feasible. In aqueous precipitation reactions of calcium phosphates that use poorly soluble calcium hydroxide as a reactant the available free calcium ions in solution at any time is small, and this will be the rate limiting step of formation of the apatite phase. The quantity of carbonate ions in the reaction solution at any time does not therefore need to be high and it is envisaged that continuously flowing a waste gas containing significantly less CO<sub>2</sub> through the phosphoric acid reactant during synthesis, analogous to process CO<sub>2</sub>-ii, would provide sufficient carbonate ions to the reaction. Alternatively, using a waste gas containing less CO<sub>2</sub> direct from a power plant to carbonate reaction water, used to make the phosphoric acid solution, under pressure could maximise the carbonate ion content. A potential translation of the work reported here would be to develop a continuous synthesis process. Such processes have been reported recently to synthesise carbonate-containing apatites, such as a continuous hydrothermal flow synthesis that produced a single phase carbonate-substituted apatite that contained 5 wt% carbonate, using urea as a carbonate source<sup>40</sup>.

#### 4. Conclusions

A sodium-carbonate co-substituted hydroxyapatite that contained 14.0 wt% carbonate was successfully prepared by an aqueous precipitation reaction utilising a non-carbonate sodium source (NaCl) in the synthesis. The bulk of the incorporated carbonate originated from a gaseous stream of CO<sub>2</sub> which was bubbled into the reactant mixture during precipitation to explore the possibility of utilising CO<sub>2</sub> gas obtained using post-combustion carbon capture (PC-CC) techniques in the preparation of the apatite rather than simply sequestering this gas in a designated reservoir. Substitution of these carbonate groups, as well as the assumed substitution of sodium groups, into the apatite structure resulted in changes in the crystal structure, particularly an increase in the *c* unit cell parameter. This high level of carbonate incorporation nearly rivalled that of an apatite prepared with sodium carbonate, Na<sub>2</sub>CO<sub>3</sub>, in non-carbonated water following the same methodology, which displayed a level of carbonate incorporation of 17.4 wt%. These results are an important first step in the development of a new manufacture route for carbonated hydroxyapatites, which have been widely used as

bone graft implants. Further, a nanoscale carbonate-substituted apatite such as that produced in this work may have potential application as a fertiliser/soil treatment if the solubility is sufficiently high. Not only is this method sensitive towards the environment, it would also improve the economics of post-combustion carbon capture as a whole.

#### 5. Conflicts of interest

There are no conflicts to declare.

#### 6. Acknowledgments

The authors would like to acknowledge the University of Aberdeen for providing financial support, the advice of Dr Jo Duncan with regards to the identification of phases from XRD and Mr Colin Taylor at the UoA School of Geosciences for support in obtaining the carbonate analysis

#### 7. References

- 1 IPCC, *Climate Change 2014: Mitigation of Climate Change*, 2014.
- 2 H. Herzog and D. Golomb, *Encycl Energy*, 2004, **1**, 1-11.
- 3 T. Wang, J. Hovland and K. J. Jens, *Journal of Environmental Sciences*, 2015, **27**, 276-289 (DOI:<https://doi.org/10.1016/j.jes.2014.06.037>).
- 4 I. Sreedhar, T. Nahar, A. Venugopal and B. Srinivas, *Renewable and Sustainable Energy Reviews*, 2017, **76**, 1080-1107 (DOI:<https://doi.org/10.1016/j.rser.2017.03.109>).
- 5 J. Blamey, E. J. Anthony, J. Wang and P. S. Fennell, *Progress in Energy and Combustion Science*, 2010, **36**, 260-279 (DOI:<http://dx.doi.org/10.1016/j.pecs.2009.10.001>).
- 6 M. Erans, V. Manovic and E. J. Anthony, *Appl. Energy*, 2016, **180**, 722-742 (DOI:<http://dx.doi.org/10.1016/j.apenergy.2016.07.074>).
- 7 J. C. Abanades and D. Alvarez, *Energy Fuels*, 2003, **17**, 308-315.
- 8 P. Huttenhuis, A. Roeloffzen and G. Versteeg, *CO<sub>2</sub> Capture and Re-use at a Waste Incinerator*, 2016.
- 9 J. Morrison, G. Jauffret, J. L. Galvez-Martos and F. P. Glasser, *Cem. Concr. Res.*, 2016, **85**, 183-191 (DOI:10.1016/j.cemconres.2015.12.016).
- 10 E. Landi, G. Celotti, G. Logroscino and A. Tampieri, *J. Eur. Ceram. Soc.*, 2003, **23**, 2931-2937 (DOI:10.1016/S0955-2219(03)00304-2).
- 11 R. Z. LeGeros, O. R. Trautz, E. Klein and J. P. LeGeros, *Experientia*, 1969, **25**, 5.



- 12 I. R. Gibson and W. Bonfield, *J. Biomed. Mater. Res.*, 2002, **59**, 697-708 (DOI:10.1002/jbm.10044).
- 13 J. A. Stephen, C. Pace, J. M. S. Skakle and I. R. Gibson, *Comparison of carbonate hydroxyapatite with and without sodium Co-substitution*, 2007.
- 14 E. Pusparini, I. Sopyan, H. Mohd and R. Singh, *Sodium-doped hydroxyapatite nanopowder through sol-gel method: Synthesis and characterization*, 2011.
- 15 M. Vignoles, G. Bonel and R. A. Young, *Calcif. Tissue Int.*, 1987, **40**, 64-70 (DOI:10.1007/BF02555707).
- 16 J. Whyte, D. Hadden, I. R. Gibson and J. Skakle, *Synthesis and stability of potassium/carbonate co-substituted hydroxyapatites*, Trans Tech Publ, 2008.
- 17 Z. Z. Zyman and M. V. Tkachenko, *Processing and Application of Ceramics*, 2013, **7**, 153-157.
- 18 D. Shi, *Introduction to Biomaterials*, World Scientific & Imperial College Press, 2005.
- 19 A. Jilavenkatesa and R. A. Condrate Sr., *J. Mater. Sci.*, 1998, **33**, 4111-4119.
- 20 A. Afshar, M. Ghorbani, N. Ehsani, M. R. Saeri and C. C. Sorrell, *Mater Des*, 2003, **24**, 197-202 (DOI:[http://dx.doi.org/10.1016/S0261-3069\(03\)00003-7](http://dx.doi.org/10.1016/S0261-3069(03)00003-7)).
- 21 J. F. Conn and L. A. Jessen, *Process for producing Hydroxyapatite*, 1980.
- 22 K. Sudarsanan and R. A. Young, *Acta Cryst.*, 1969, **B25**, 1534-1543.
- 23 S. N. Danilchenko, A. V. Koropov, I. Y. Protsenko, B. Sulkio-Cleff and L. F. Sukhodub, *Cryst Res Technol*, 2006, **41**, 268-275 (DOI:10.1002/crat.200510572).
- 24 Y. Kitano, M. Okumura and M. Idogaki, *Geochem. J.*, 1975, **9**, 75-84 (DOI:10.2343/geochemj.9.75).
- 25 I. Rehman and W. Bonfield, *J. Mater. Sci. Mater. Med.*, 1997, **8**, 1-4 (DOI:10.1023/A:1018570213546).
- 26 A. Grunenwald, C. Keyser, A. M. Sautereau, E. Crubézy, B. Ludes and C. Drouet, *J. Archaeol. Sci.*, 2014, **49**, 134-141 (DOI:10.1016/j.jas.2014.05.004).
- 27 S. Raynaud, E. Champion, D. Bernache-Assollant and P. Thomas, *Calcium phosphate apatites with variable Ca/P atomic ratio I. Synthesis, characterisation and thermal stability of powders*, 2002.
- 28 Y. X. Pang and X. Bao, *Journal of the European Ceramic Society*, 2003, **23**, 1697-1704 (DOI:[https://doi.org/10.1016/S0955-2219\(02\)00413-2](https://doi.org/10.1016/S0955-2219(02)00413-2)).
- 29 M. E. Fleet, *Biomaterials*, 2009, **30**, 1473-1481 (DOI:<https://doi.org/10.1016/j.biomaterials.2008.12.007>) View Article Online (DOI:10.1039/C7TA09334A)
- 30 T. I. Ivanova, O. V. Frank-Kamenetskaya and A. B. Kol'tsov, *Z. Kristallogr.*, 2004, **219**, 479-486 (DOI:10.1524/zkri.219.8.479.38332).
- 31 M. Figueiredo, A. Fernando, G. Martins, J. Freitas, F. Judas and H. Figueiredo, *Ceram. Int.*, 2010, **36**, 2383-2393 (DOI:<https://doi.org/10.1016/j.ceramint.2010.07.016>).
- 32 E. A. P. De Maeyer, R. M. H. Verbeeck and D. E. Naessens, *Inorg. Chem.*, 1993, **32**, 5709-5714.
- 33 E. A. P. De Maeyer, R. M. H. Verbeeck and D. E. Naessens, *Inorg. Chem.*, 1994, **33**, 5999-6006.
- 34 R. D. Shannon, *Acta Crystallogr. Sect. A Found. Crystallogr.*, 1976, **32**, 751-767 (DOI:10.1107/S0567739476001551).
- 35 M. I. Kay, R. A. Young and A. S. Posner, *Nature*, 1964, **204**, 1050-1052 (DOI:10.1038/2041050a0).
- 36 A. S. Posner, A. Perloff and A. F. Diorio, *Acta Cryst.*, 1958, **11**.
- 37 E. Garskaite, K. Gross, S. Yang, T. C. Yang, J. Yang and A. Kareiva, *CrystEngComm*, 2014, **16**, 3950-3959.
- 38 J. Barralet, S. Best and W. Bonfield, *J. Mater. Sci. Mater. Med.*, 2000, **11**, 719-724.
- 39 Q. Liu, J. P. Matinlinna, Z. Chen, C. Ning, G. Ni, H. Pan and B. W. Darvell, *Ceram. Int.*, 2015, **41**, 6149-6157 (DOI:<https://doi.org/10.1016/j.ceramint.2014.11.062>).
- 40 A.A. Chaudhry, J.C. Knowles, I. Rehman and J.A. Darr, *J. Biomater. Appl.* 2012, **28**, 448-461 (DOI: 10.1177/0885328212460289)